Absorption near band edges in heavily doped GaAs

W. Sritrakool*
Physics Department, University of Ottawa, Ottawa, Ontario, Canada K1N 6N5

V. Sa-yakanit
Physics Department, Chulalongkorn University, Bangkok 10500, Thailand

H. R. Glyde
Physics Department, University of Delaware, Newark, Delaware 19716
(Received 11 February 1985)

The optical-absorption coefficient $\alpha(\omega)$ in heavily doped n- and p-type GaAs is evaluated for comparison with the observed values of Casey *et al.* The purpose is to test the theory of electrons in heavily disordered systems derived by Sa-yakanit and the absorption matrix element (ME) which follows from this theory. The present calculation of $\alpha(\omega)$ begins with the density of electron states (DOS) and the electron wave functions. The ME is then derived. The screening of the interactions by the carrier electrons depends on the DOS. Since the DOS, ME, screening, and the Fermi energy, which provide the essential input for $\alpha(\omega)$, are interdependent they must be evaluated iteratively until consistent. The final $\alpha(\omega)$ agrees quite well with experiment. The overall $\alpha(\omega)$ is also similar to that calculated by Casey and Stern although very different inputs for $\alpha(\omega)$ are used. The $\alpha(\omega)$ is found to be very sensitive to the DOS, the ME, and the band-gap shrinkage. The comparison with experiment suggests the present combined model of the DOS and the ME represent heavily doped GaAs well but that the band-gap-shrinkage calculations need further refinement.

I. INTRODUCTION

Optical absorption and transport in heavily doped semiconductors has been an active field of research for over 25 years. This interest, which has been exhaustively reviewed by Abram *et al.*,[1] by Redfield,[2] and by Efros,[3] is motivated largely by the development of semiconductor lasers and Esaki diodes. Here we present a specific calculation of the optical-absorption coefficient $\alpha(\omega)$ near band edges in heavily doped GaAs at $T=297$ K. The aim is to test a recently developed theory[4-7] of the densities of carrier states $\rho(E)$ in the band-tail region and the absorption matrix element (ME) that follows from this theory. The new ME is developed in the present paper. The interdependent $\rho(E)$, ME, Fermi energy, and screening provide an internally consistent model for $\alpha(\omega)$ which can be tested by comparison with experiment. GaAs is considered because of the relative simplicity of its band structure and because both experimental measurements[8] and previous[9] calculations are available for comparison.

Any calculation of $\alpha(\omega)$ is necessarily complicated. A model must include a description of the band structure and the density of carrier states under heavy doping. The interaction between the carriers and the dopant ions must be considered. The wave functions of the carriers and a model for the ME using these wave functions is required. The screening of the interactions by the carriers, the Fermi energy, and the variation of the band gap with doping must be also determined.

The present model begins with pure GaAs having a single conduction band separated from a doubly degenerate valence band by an energy gap E_g. Below the doubly degenerate valence band there is another "split-off" valence band which we ignore. Since absorption near band edges only is considered the bands are assumed to be parabolic with an appropriate effective mass. This restricts the investigation to a narrow range of energies, $1.35\ \text{eV} \leq \hbar\omega \leq 1.55$ eV. We also consider "vertical" transitions only which again restricts us to GaAs where the conduction- and valence-band edges lie directly above one another.

When GaAs is doped with impurities of positive charge Z (relative to GaAs) the electrons donated by the impurities occupy states immediately below the conduction band. At heavy-doping levels, $N_D \geq 10^{18}$ cm^{-3}, these impurity electron states merge with the conduction band and form a conduction-band tail reaching into the energy gap.[1,10,11] The impurity electrons are here assumed to interact with the impurity ions via a screened Coulomb potential. Screening is described within the Thomas-Fermi approximation. As pointed out by Wolff,[12] the average (Hartree) electron-electron and electron-ion potentials cancel due to charge neutrality. The impurity electron-band-tail states are therefore determined by fluctuations in the electron-impurity ion potential which follow from local fluctuations in the impurity-ion concentration.

Similarly, when the doping impurities have a negative Z, hole (acceptor) states appear above the valence band. At doping levels $N_A \geq 10^{18}$ cm^{-3} these hole states form a valence-band tail reaching up into the energy gap. A specific example of band tails in both the valence and conduction bands calculated here for $N_A = 1.5\times10^{18}$ cm^{-3}, $N_D = 3\times10^{17}$ cm^{-3} giving $p = N_A - N_D = 1.2\times10^{18}$ cm^{-3} is shown in Fig. 1. For both positive and negative impurities we assume "shallow" impurity states so that at high doping the impurity states always form band tails.

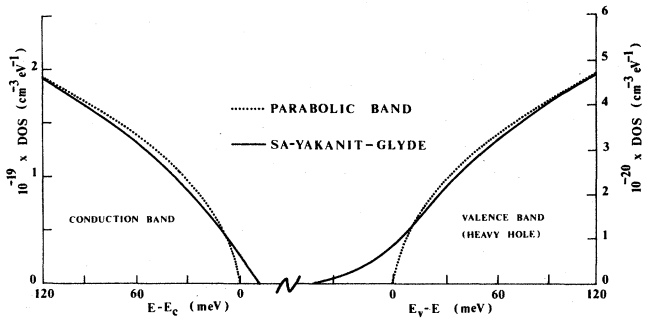

FIG. 1. Sa-yakanit-Glyde (SG) density of states (DOS) in the valence and conduction bands of p-type GaAs [Eq. (3) in the text]. The doping levels are $N_A=1.5\times10^{18}$ cm^{-3}, $N_D=3\times10^{17}$ cm^{-3}, $p=N_A-N_D=1.2\times10^{18}$ cm^{-3}, and E_V and E_c are the valence- and conduction-band edges, respectively.

A central approximation in the present model is the neglect of electron-hole interactions. While this (exciton) interaction is very important in pure[1,13] GaAs, the strong screening of the electron-hole interaction by the carriers (electrons and holes) is assumed to reduce its importance in the heavy-doping limit substantially. This restricts the model to the heavy-doping limit. Also if the doping is heavily compensated ($N_A\approx N_D$) so that there is no net carrier concentration to provide screening, the electron-hole interaction becomes important.[14] Thus we must avoid strongly compensated doping here. The present model also uses the heavy-doping limit ($N_{D,A}^{1/3}a\gg1$ where a is a typical Bohr orbit radius of a carrier) to obtain $\rho(E)$. In this limit each carrier interacts with many impurities and the carrier-impurity interaction fluctuates in strength throughout the semiconductor depending upon the local concentration of impurities.

Heavy-impurity doping also causes the gap, E_g, between the valence and the conduction band to shrink. This shifts the absorption to lower energy. This band-gap shrinkage ΔE_g is due chiefly to the (negative) exchange energy of the added impurity electrons.[1] However, there are several other high-order contributions which are difficult to evaluate with confidence. Here we describe the band-gap shrinkage using an empirical expression developed by Casey and Stern[9] and by a more fundamental expression due to Inkson.[15] While the band-gap shrinkage shifts $\alpha(\omega)$ to lower ω, the rise of the Fermi level E_F into the conduction band on heavy doping shifts the absorption to higher energy (the Moss-Burstein shift[16,17]). Thus ΔE_g and the Moss-Burstein shift tend to compensate for each other. To identify the effect of ΔE_g alone we also present results with ΔE_g set arbitrarily to zero.

Kane[18] and Bonch-Bruevich[19] first derived a semiclassical density of states (DOS) in the low-energy band-tail region. This was extended to a full quantum theory by Halperin and Lax.[20] These theories are thoroughly reviewed by Abram *et al.*[1] Since these reviews Sa-yakanit[4,5] and Sa-yakanit and Glyde[6] (SG) developed a theory using the full quantum ideas of Halperin and Lax which takes advantage of the Feynman path-integral method. They were able to obtain an analytic expression for the density of states $\rho(E)$ over the whole energy range E.

In the SG theory, the fluctuation seen by an electron (or hole) due to the impurities is modeled by a harmonic well. The curvature of this well depends upon the electron (hole) energy in the band and is found using the Lloyd-Best[21] variational principle. Carrier states deep in the band tail (low E) arise from deep, sharply parabolic harmonic wells. The ground-state wave function of a particle in a harmonic well is a Gaussian function. Thus we use Gaussian wave functions to describe carrier states in the absorption matrix element appearing in $\alpha(\omega)$. Once the model-impurity harmonic well is determined variationally at each carrier energy both the DOS and the wave functions to be used in the matrix element are determined. In an earlier publication[22] we evaluated the screening length Q^{-1} in the Thomas-Fermi approximation and the Fermi energy E_F in heavily doped n-type GaAs using the SG density of states. These calculations showed that Q is not greatly sensitive to the specific form of $\rho(E)$ in the band-tail region. This is because the total number of states in the band tail is small compared to the number of states higher in the band.

The only direct measurement of $\rho(E)$ for heavily doped p-type GaAs is the Schottky junction tunneling result of Mahan and Conley.[23] We show later in this paper that the SG $\rho(E)$ agrees well with the Mahan and Conley measurements. Takeshima[24] has derived a $\rho(E)$ using a Green-function technique which also agrees well with the Mahan and Conley data. Unfortunately, while the Mahan and Conley results demonstrate band tailing clearly, the data is not discriminating and any reasonable treatment of band tailing (such as Kane's original[18] semiclassical approximation) will agree with it.

A central aim here is therefore to test the SG $\rho(E)$ and the ME that follows from it by calculating $\alpha(\omega)$. In the present model, the $\rho(E)$, the matrix element, the screening length Q^{-1}, and the Fermi energy are all interdependent and must be determined iteratively until consistent. The model therefore has substantial internal consistency which removes some of the possible choice of model parameters. Comparison with experiment provides a global test of the complete model.

In the Sec. II we present the expression for $\alpha(\omega)$ and the SG DOS used in the present calculation. We then present the new initial- and final-state wave functions for the absorption transition which are associated with the initial and final energy states in $\rho(E)$. The transition matrix element is evaluated and shown to approach correct asymptotic values. The evaluation of the band-gap shrinkage is also discussed.

In Sec. III we present the absorption coefficient for both p- and n-type GaAs with and without band-gap shrinkage. The sensitivity of $\alpha(\omega)$ to the DOS is also tested. In the Sec. IV we discuss the DOS and $\alpha(\omega)$.

II. OPTICAL-ABSORPTION COEFFICIENT

A. Absorption

Optical absorption can be readily described[25] using a "one-electron" approximation. In this picture, once the

density of states has been determined, incoming photons are absorbed by exciting noninteracting electrons from states in a valence band i to states in a conduction band. This gives a coefficient, in cgs units, of[26]

$$\alpha_i(\omega)=\frac{4\pi^2e^2\Omega}{m_0^2cn\omega}\int_{-\infty}^{\infty}dE\,\rho_{vi}(E)\rho_c(E')M(E,E')^2 \times[f(E)-f(E')]\ , \quad (1)$$

where $E'=E+\hbar\omega$, ω is the photon frequency, e and m_0 are the electron charge and mass, respectively. The n, c, and Ω are the refractive index, velocity of light, and volume of the (pure) crystal, respectively, and $f(E)$ is the Fermi-Dirac distribution function. The $\rho_{vi}(E)$ and $\rho_c(E)$ are the SG DOS's for a single spin per unit volume in the valence i and conduction bands, respectively. $M(E,E')$ is the effective matrix element of the momentum operator for transitions between states in the valence band i at energy E and states in the conduction band at energy E'. When there are degenerate valence bands, as in GaAs, the total $\alpha(\omega)$ is a sum over each i. Also, since there is no spin flip possible in the transition, spin degeneracy is included by multiplying $\rho_{vi}(E)$ by 2. Therefore

$$\alpha(\omega)=2\sum_{i=1}^{2}\alpha_i(\omega)\ . \quad (2)$$

We now examine the basic ingredients of $\alpha(\omega)$: the DOS, the Fermi energy in $f(E)$, the ME, and the band-gap shrinkage ΔE_g.

B. Density of states

The density of states for carriers in a heavily doped semiconductor is obtained by treating a carrier as a particle in a disordered system. The disorder is created by the randomly located impurities in a host having a constant static dielectric function ϵ_0. The low-energy electron states in the band tail are obtained when fluctuations leading to dense clusters of impurities create deep attractive potential wells.

As noted above, Kane[18] and Bonch-Bruevich[19] independently obtained a $\rho(E)$ from this model in a semiclassical approximation. Since the (positive) kinetic energy of localization of the carriers in the deep well was ignored, their result underestimated the carrier energy and predicted too many carriers having low energy (too large a band tail). This problem was corrected by Halperin and Lax[20] using a full quantum-mechanical treatment. However, their $\rho(E)$ is obtained as a numerical table and is not easy to use. Sa-yakanit,[5] following Halperin and Lax's ideas, was able to obtain an expression for $\rho(E)$ valid at all E. This expression[5,6] reduces to a simple form in the band-tail region (low E) and reduces to the expected parabolic value at high E. However, it is quite complicated at intermediate E, too complicated to use conveniently. At low E, the simple tail DOS, $\rho_T(E)$, agrees well with Halperin and Lax's result.[6] The $\rho_T(E)$ can also be extended to high enough E that it crosses the Kane DOS, $\rho_K(E)$, which is valid at higher energies.

The DOS we use here, denoted the SG (Refs. 6 and 7) DOS, consists of the tail DOS $\rho_T(E)$ up to the energy E^* at which it crosses $\rho_K(E)$. Thereafter $\rho_K(E)$ is used, i.e.,

$$\rho(E)=\rho_T(E)[1-\Theta(E-E^*)]+\rho_K(E)\Theta(E-E^*)\ , \quad (3)$$

where $\Theta(x)$ is the Heaviside step function. Kane's DOS for a band having effective mass m^* is[6]

$$\rho_K(E)=\frac{m^{*3/2}}{4\pi^2\hbar^3}\xi_Q^{1/4}e^{-(E-E_0)^2/4\xi_Q} \times D_{-3/2}(-(E-E_0)/\sqrt{\xi_Q})\ , \quad (4)$$

where E_0 is the mean and $\xi_Q=2\pi Z^2e^4N/Q\varepsilon_0^2$ is the variance of the fluctuating impurity potential. In (4) $D_P(x)$ is the parabolic cylinder function and N is the number of impurities of charge Z. Equation (4) can be expressed in terms of the dimensionless energy $\nu=(E_0-E)/E_Q$ where $E_Q=\hbar^2Q^2/2m^*$ as

$$\rho_K(\nu)=\frac{1}{8\sqrt{2}\pi^2}\xi'^{9/4}e^{-\nu^2/4\xi'}D_{-3/2}(\nu/\sqrt{\xi'})\ , \quad (5)$$

where $\xi'=\xi_Q/E_Q^2$ and $\rho_K(E)$ is now in units of $Q^3/E_Q\xi'^2$.

The $\rho_T(E)$ is obtained from Eq. (2) of Ref. 7. In the same units as in (5), this is

$$\rho_T(\nu,z)=\xi'^{3/4}\frac{a(\nu,z)}{b(\nu,z)^{3/4}}e^{-b(\nu,z)/4\xi'} \times D_{3/2}([b(\nu,z)/\xi']^{1/2})\ , \quad (6)$$

where $a(\nu,z)$ and $b(\nu,z)$ are dimensionless universal functions defined in Eq. (4) of Ref. 7. The $z(\nu)$ is the variational parameter which is determined at each carrier energy E [$\nu=(E_0-E)/E_Q$] using the Lloyd and Best[21] variational principle. Numerical results for $\rho_T(E)$, $\rho_K(E)$, and Halperin and Lax's DOS have been presented in Ref. 7. Values of $\rho(E)$ given by (3) for GaAs are shown in Fig. 1. In Fig. 1 the scales for the conduction and valence bands differ and $\rho(E)$ for the conduction band is significantly smaller than that in the valence band.

C. Screening and Fermi energy

In $\alpha(\omega)$ we need the Fermi energy E_F [to be used in the Fermi function $f(E)$] and the screening length Q^{-1}. From (5) and (6), $\rho(E)$ also depends on Q. Previously[22] we calculated both E_F and Q in n-type GaAs using (3). We follow the same procedure here for both n- and p-type GaAs. In the case of the p-type GaAs, E_F is determined using

$$p=\sum_i\int_{-\infty}^{\infty}\rho_{vi}(E)f_h(E)dE\ , \quad (7)$$

where p is the net hole concentration (normally set at $p=N_A-N_D$). Q^2 is obtained from

$$Q^2=\sum_i\frac{4\pi e^2}{\epsilon_0}\int_{-\infty}^{\infty}\rho_{vi}(E)\left[-\frac{\partial f_h(E)}{\partial E}\right]dE\ . \quad (8)$$

We calculated E_F and Q here via (7) and (8) for both p- and n-type GaAs at $T=297$ K using the SG DOS [Eq.

(3)], the Kane DOS [Eq. (4)], and the well-known parabolic DOS. In the former two cases, Eqs. (7), (8), and the DOS must be evaluated iteratively until consistent. To model the parabolic bands we used $m_e=0.066m_0$ for the conduction band, and $m_{hh}=0.55m_0$ and $m_{hl}=0.085m_0$ for the heavy-hole and light-hole valence bands, respectively. These values of the effective masses (and the doping concentrations) were taken from Casey and Stern[9] so that we may compare our absorption coefficients with theirs. The results are displayed in Table I and show that Q is insensitive to the DOS. However, E_F is quite sensitive to $\rho(E)$.

D. Matrix element

The matrix element appearing in $\alpha(\omega)$ is[26]

$$M(E,E')=\int_\Omega d\mathbf{r}\,\phi_c^*(\mathbf{k}_c,\mathbf{r})(\hat{\mathbf{e}}\cdot\mathbf{p})\phi_v(\mathbf{k}_v,\mathbf{r}) , \tag{9}$$

where $\mathbf{p}$ is the carrier momentum operator and $\hat{\mathbf{e}}$ is a unit vector in the direction of the incoming photon. As discussed by Kohn,[27] the wave function $\phi(\mathbf{k},\mathbf{r})$ of a carrier near the band extremum ($\mathbf{k}\approx 0$) may be written as a product of a Bloch function $u(\mathbf{r})$ ($\mathbf{k}=0$) and a slowly varying envelope function $\varphi(\mathbf{r})$, i.e., $\phi_c(\mathbf{k}_c,\mathbf{r})=\varphi_c(\mathbf{r})u(\mathbf{r})$. Using the property that each $\varphi(\mathbf{r})$ is slowly varying with $\mathbf{r}$, the $M(E,E')$ may be separated into a Bloch term and an envelope term,

$$M(E,E')=M_bM_{\rm env}$$

where

$$M_{\rm env}=\int d\mathbf{r}\,\varphi_c^*(\mathbf{r})\varphi_v(\mathbf{r}) \tag{10}$$

and

$$M_b=\frac{1}{\Omega}\int d\mathbf{r}\,u_c^*(\mathbf{r})(\hat{\mathbf{e}}\cdot\mathbf{p})u_v(\mathbf{r}) .$$

Squaring and averaging $M(E,E')$ over all directions gives,

$$M(E,E')^2=M_b^2M_{\rm env}^2 . \tag{11}$$

An expression for M_b^2 has been derived by Kane[28] for transitions between p- and s-like Bloch functions using perturbation theory. For all III-V semiconductors, this is

$$M_b^2=1.25\frac{m_e^2P^2}{6\hbar}\simeq 1.25\frac{m_0^2E_g}{12m_e}\left[\frac{E_g+\Delta}{E_g+\frac{2}{3}\Delta}\right] , \tag{12}$$

where P is the ME defined by Kane. In GaAs at room temperature the energy gap is $E_g=1.424$ eV and the spin-orbit splitting is $\Delta=0.33$ eV. More recent studies[29] find that the M_b^2 is 25% larger than the value used previously.[9] We have accordingly increased (12) by a factor of 1.25 and used this single increased value of M_b^2 in all calculations of $\alpha(\omega)$.

Several values of $M_{\rm env}$ have been used in the past. Eagles,[30] for example, assumed a localized acceptor wave function φ_v of hydrogenic form and a delocalized acceptor function φ_c of plane wave form. This gives

$$|M_{\rm env}|^2=\frac{64\pi a^3\Omega^{-1}}{(1+a^2k_c^2)^4} \tag{13}$$

where a is the Bohr radius. For transitions right at the band edge ($k_c=0$) this $|M_{\rm env}|^2$ becomes simply $(64\pi a^3/\Omega)$. This band-edge value is often used as simple constant model ME for all transitions. Casey and Stern[9] use envelope wave functions for all states of the form

$$\varphi(\mathbf{r})=(\beta^3/\pi)^{1/2}\exp(i\mathbf{k}\cdot\mathbf{r})\exp(-\beta|\mathbf{r}-\mathbf{r}_i|) ,$$

where β and k are energy-dependent parameters and $\mathbf{r}_i$ is the impurity location. In the SG theory the potential wells seen by the carriers due to the impurities are modeled by harmonic wells. The curvature of the wells ($m\omega^2$) is an energy-dependent variational parameter; related to $z(E)$ by $\hbar\omega=2E_Q/z^2$. In this model the kinetic energy of localization is $T=\frac{3}{4}\hbar\omega=\frac{3}{2}E_Q/z^2$. The ground-state wave function of a particle in a harmonic well is a Gaussian and at low E only ground states are included in $\rho(E)$. Thus it is natural (see the Appendix) to use Gaussian envelope functions of the form

$$\varphi(\mathbf{r})=\left[\frac{2\gamma}{\pi}\right]^{3/4}\exp(i\mathbf{k}\cdot\mathbf{r})\exp[-\gamma(\mathbf{r}-\mathbf{r}_i)^2] \tag{14}$$

for energies up to where the carrier ceases to be localized. Here $\gamma(E)$ is the energy-dependent Gaussian parameter, $\gamma(E)=m\omega/\hbar=mQ^2/z^2$ and k is determined as discussed below. On substituting $\varphi(\mathbf{r})$ in (10), and averaging the $\mathbf{r}_i$ over all random impurity positions we obtain[31]

$$|M_{\rm env}|^2=\frac{1}{\Omega}\left[\frac{2\pi}{\gamma_v+\gamma_c}\right]^{3/2}\left[\frac{\gamma_v+\gamma_c}{k_ck_v}\right]\sinh\left[\frac{k_ck_v}{\gamma_v+\gamma_c}\right]\times e^{-(k_c^2+k_v^2)/2(\gamma_v+\gamma_c)} . \tag{15}$$

This ME is a substantially simpler than that obtained us-

TABLE I. Self-consistent results for heavily doped GaAs at $T=297$ K using the Sa-yakanit-Glyde (SG) density of states. The effective masses used are $m_e=0.066m_0$, $m_{hh}=0.55m_0$, and $m_{hl}=0.085m_0$. N_D and N_A are the donor and acceptor concentrations. Q^{-1} is the screening length. E_F-E_v and E_F-E_c are Fermi energies measured away from the valence- and conduction-band edges, respectively. ξ_Q is the potential fluctuation parameter defined in Eq. (4).

p-type GaAs						n-type GaAs					
N_D (cm^{-3})	N_A (cm^{-3})	Q (cm^{-1})	Q^{-1} (A)	E_v-E_F (meV)	$\xi_Q^{1/2}$ (meV)	N_D (cm^{-3})	N_A (cm^{-3})	Q (cm^{-1})	Q^{-1} (A)	E_F-E_c (meV)	$\xi_Q^{1/2}$ (meV)
3.0×10^{17}	1.5×10^{18}	2.49×10^6	40.2	−70.2	23.3	2.5×10^{18}	5.0×10^{17}	2.06×10^6	48.5	82.8	33.2
6.0×10^{17}	3.0×10^{18}	3.45×10^6	29.0	−47.5	28.1	4.1×10^{18}	8.0×10^{17}	2.30×10^6	43.4	121.0	40.1
4.0×10^{18}	2.0×10^{19}	7.47×10^6	13.4	33.7	49.3	8.4×10^{18}	1.7×10^{18}	2.64×10^6	37.9	198.0	53.8

ing hydrogenic envelope functions.[9] It also has correct asymptotic limits. For example, for transitions between states far from the band edges (delocalized states) both γ_c and γ_v go to zero. In this limit

$$|m_{\text{env}}|^2=\frac{2\pi^2}{\Omega k_c k_v}\delta(k_v-k_c)$$
$$=\frac{(2\pi)^3}{\Omega}\delta(\mathbf{k}_v-\mathbf{k}_c)\,, \tag{16}$$

which is the result expected for two plane-wave, delocalized carrier states. Similarly, for a transition from a localized state near the valence-band edge ($k_v=0,\gamma_v\neq 0$) to a delocalized state high in the conduction band ($k_c\neq 0,\gamma_c=0$) we find (15) becomes

$$|M_{\text{env}}|^2=\frac{1}{\Omega}\left[\frac{2\pi}{\gamma_v}\right]^{3/2}e^{-k_c^2/2\gamma_v}\,. \tag{17}$$

For transitions right at the band edge ($k_c=0$) we obtain a constant ME,

$$|M_{\text{env}}|^2=(2\pi/\gamma_v)^{3/2}\frac{1}{\Omega}=\frac{64\pi}{\Omega}\pi^{1/2}\left[\frac{z_v}{2Q}\right]^3 \tag{18}$$

which may be compared to Eagles's constant matrix element describing the same transition.

As noted above $\gamma_v=mQ^2/z_v^2$ ($m=m_{hl}$ or m_{hh}) and $\gamma_c=m_eQ^2/z_c^2$ are determined directly by the variational parameters $z_v(E)$ and $z_c(E)$ appearing in the band-tail density of states, $\rho_T(E)$. However, for energies $E>E^*$ in (3), where the Kane density of states is used, the z is not known. For $E>E^*$ we have determined z by a simple linear extrapolation from $z(E)$ for $E<E^*$ using the physical idea that the localization energy $T=\frac{3}{2}E_Q/z^2$ must vanish at high energy E. Typical values of z and T (in units of E_Q) for the light hole ($m=m_{hl}$) valence band in GaAs with $p=1.2\times10^{18}$ cm^{-3} are shown in Fig. 2.

To determine k_v and k_c we have followed two methods. Firstly, we have used the concept of a well-defined "mobility edge" E_m in Anderson's theory[32] of localization and of separable bands[33] above and below E_m. Below E_m we simply assume a completely localized band and set $k=0$. Above E_m we assume a free-particle band with k given by the parabolic band relation $\hbar k=[2m(E-E_m)]^{1/2}$. Since the choice of the E_m is not clear, we take them at the nominal band edges, $E_{mc}=E_c=E_g$ and $E_{mv}=E_v=0$. This choice is depicted graphically in Fig. 3.

Secondly, we use the counting method proposed by Casey and Stern.[9] In this method we determine k_c at energy E, for example in the conduction band, by counting the number of states per unit volume, $N(E)/\Omega$, occupied up to energy E in the band using the real $\rho_c(E)$. We then assume a parabolic density of states for which there is a well-defined relation between k, E, and $N(E)$. The k_c value is that value of k needed to accomodate the number of states $N(E)/\Omega$ in the assumed parabolic density, i.e.,

$$N(E)/\Omega=\int_{-\infty}^{E}\rho_c(E')dE'=\left[\frac{4\pi}{3}\right]k_c^3/(2\pi)^3\,. \tag{19}$$

Similarly, for the valence band

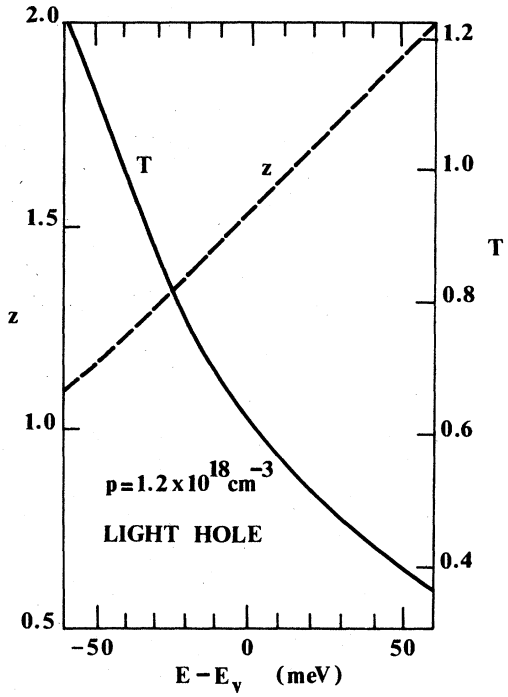

FIG. 2. Variational parameter, $z=(\hbar\omega/2E_Q)^{-1/2}$, describing the curvature of the model harmonic wells ($m^*\omega^2$) seen by the carriers due to impurities. Here $E_Q\equiv\hbar^2Q^2/2m^*$ where Q is the inverse screening length [$Q=0.025$ Å^{-1} from Eq. (8)]. $T=\frac{3}{4}\hbar\omega/E_Q=\frac{3}{2}/z^2$ is the kinetic energy of localization (in units of E_Q) which vanishes at high energy $E-E_v$. The light-hole valence band is considered ($m^*=m_{hl}=0.085m_0$) at $p=1.2\times10^{-18}$ cm^{-3}.

$$k_v=\left[6\pi^2\int_E^{\infty}\rho_v(E')dE'\right]^{1/3}\,. \tag{20}$$

We found that $\alpha(\omega)$ was insensitive to the method of determining k_c and k_v for the choice of $E_{mc}=E_c$ and $E_{mv}=E_v$.

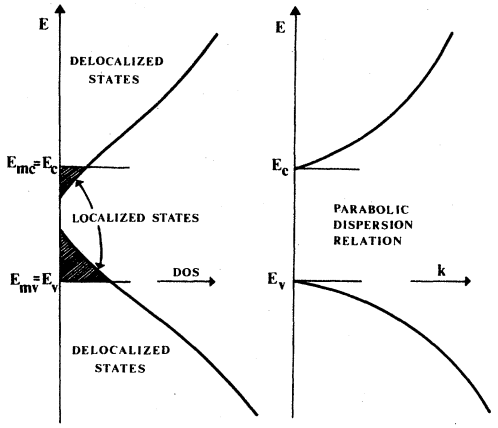

FIG. 3. Schematic representation of the band structure showing (on the left) localized states between E_v and E_c and delocalized states outside this range. On the right the parabolic DOS used to describe the delocalization states above the mobility edge $E_{mc}=E_c$ and below $E_{mv}=E_v$ is shown.

E. Band-gap shrinkage

Heavy doping has two important effects on the bands in addition to band tailing. Firstly, there is a rigid shift downward of all the bands by an amount E_0 due to the positive donor ions. Halperin and Lax[20] give an explicit expression for E_0. Since all bands are shifted equally, this shift has no direct effect on $\alpha(\omega)$. Secondly, the conduction band shrinks downward[14,15,34–40] relative to the valence band by an amount ΔE_g, due chiefly to the exchange energy of the donor electrons in the conduction band. Contributions to ΔE_g also come from the donor electron correlation energy and from lattice relaxation around the impurities. If the exchange energy is approximated by the free, unscreened electron gas-exchange energy we expect[1] $\Delta E_g \propto n^{1/3}$.

Inkson[15] has evaluated ΔE_g by calculating the relative shift of the conduction and valence band using a Thomas-Fermi model of screening. This gives

$$\Delta E_g = -\frac{2e^2 k_F}{\pi \varepsilon_0}\left\{1+\frac{Q}{k_F}\left[\frac{\pi}{2}-\tan^{-1}\left[\frac{k_F}{Q}\right]\right]\right\}, \qquad (21)$$

where the first term is the unscreened result in a medium having static dielectric constant ε_0. Abram *et al.*[1] have improved this result by using Lindhard screening. Casey and Stern[9] determined an empirical expression for ΔE_g for p-type GaAs at 297 K by fitting to observed values of $\alpha(\omega)$. This is

$$\Delta E_g = -1.6\times 10^{-8}(p)^{1/3}, \qquad (22)$$

where p is in cm^{-3} and ΔE_g is in eV. The ΔE_g due to Inkson,[21] due to Abram *et al.*,[1] using Lindhard screening, the unscreened exchange value, and Casey and Stern's empirical expression[9] are compared in Fig. 4. All curves except the Casey and Stern value are taken from Abram *et al.*[1] An accurate determination of ΔE_g is clearly difficult and is as yet an unresolved problem.[34,36]

Here we use the ΔE_g due to Inkson[15] with Q determined as discussed above, and due to Casey and Stern. From Fig. 4 it is clear that the Thomas-Fermi approximation overestimates ΔE_g and that the Casey and Stern value is likely to yield the best results for $\alpha(\omega)$.

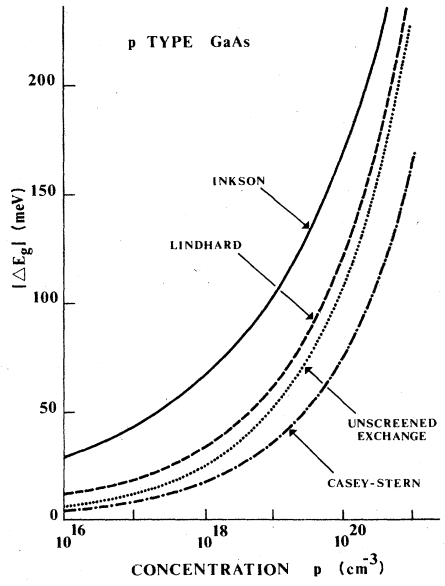

FIG. 4. Band-gap shrinkage ΔE_g in p-type GaAs calculated by Inkson (Ref. 15) using Thomas-Fermi screening, by Abram *et al.* (Ref. 1) using Lindhard screening, by Casey and Stern (Ref. 9) using an empirical fit to observed values, and as given by the unscreened exchange term.

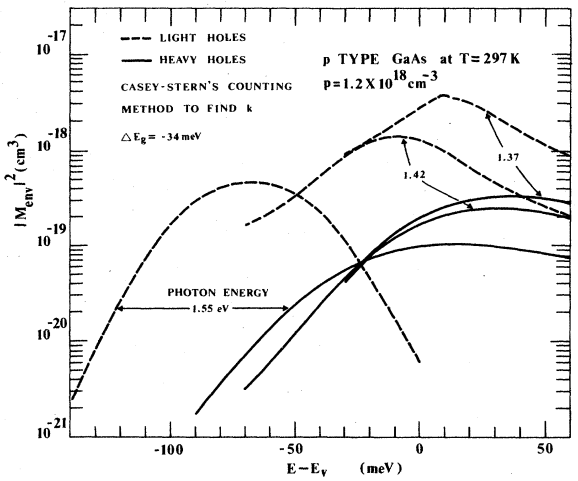

FIG. 5. Envelope matrix elements, Eq. (15), for electron excitation from the light- (dashed line) and heavy- (solid line) hole valence bands to the conduction band for three incident photon energies $\hbar\omega = 1.55$, 1.42, and 1.37 eV. The counting method proposed by Casey and Stern (Ref. 9) is used to determine k_v and k_c in $|M_{\mathrm{env}}|^2$. The energy scale is shifted by $\Delta E_g = -34$ meV.

III. RESULTS

A. Preliminary results

To introduce the results for $\alpha(\omega)$ we show in Figs. 5 and 6 the present envelope matrix element (ME) given by

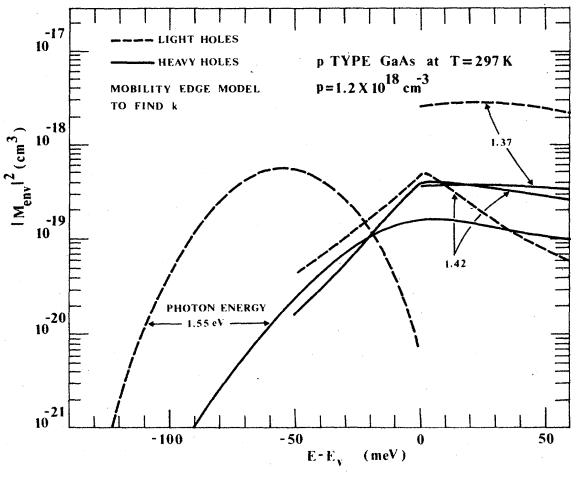

FIG. 6. As Fig. 5 with k_v and k_c determined assuming parabolic bands starting at the mobility edge (here E_v) with $\Delta E_g = 0$.

Eq. (15). In Fig. 5 the parameters k_v and k_c in $|M_{\text{env}}|^2$ are established using Casey and Stern's[9] counting method which is discussed in Eqs. (19) and (20). In Fig. 6 the k_c is established by simply assuming a well-defined mobility edge in the band. Below the mobility edge we assume $k_c=0$. Above the mobility edge we assume a parabolic energy band with k_c related to E by the usual parabolic band relation. A similar argument for the valence band determines k_v. This we call the mobility edge method. Comparing Figs. 5 and 6 we see that $|M_{\text{env}}|^2$ is quite insensitive to how k_v and k_c are determined for a photon energy of 1.55 eV. At lower photon energies the energy dependence (on $E-E_v$) of $|M_{\text{env}}|^2$ depends somewhat upon how k_v and k_c are determined. However, the magnitude of M_{env} is relatively insensitive to the method of determining k. Since $|M_{\text{env}}|^2$ appears in $\alpha(\omega)$ integrated over $(E-E_v)$ [see (1)], the final $\alpha(\omega)$ changes by only a few percent when $|M_{\text{env}}|^2$ in Fig. 5 is replaced by that in Fig. 6. Thus, with the present choice of mobility edges, it matters little whether Casey and Stern's counting method or the mobility edge method is used to determine k_c and k_v.

In Figs. 5 and 6, E is the initial energy of the excited electron in the valence band ($E'=\hbar\omega+E$). The present $|M_{\text{env}}|^2$ shown in Figs. 5 and 6 are approximately ten times smaller than those obtained by Casey and Stern. However, the present $|M_{\text{env}}|^2$ is a much broader function of $(E-E_v)$ and extends over a much wider interval of $E-E_v$. Thus when the Casey and Stern and present $|M_{\text{env}}|^2$ appear integrated over E in $\alpha(\omega)$ they give approximately the same $\alpha(\omega)$.

In Fig. 7 we show the present $\alpha(\omega)$ for both p- and n-type GaAs with the band-gap shrinkage ΔE_g arbitrarily set to zero. The purpose is to display the Moss-Burstein[16,17] shift in the calculated $\alpha(\omega)$. In Fig. 7 the calculated $\alpha(\omega)$ is shifted to higher energy, displaying a larger apparent energy gap, than the observed $\alpha(\omega)$. This is because the Fermi energy moves up in the conduction band, increasing in energy with increased doping concentration. The electrons must be excited to states above E_F so that the apparent energy gap shifts to higher E (Moss-Burstein shift) as E_F increases. With $\Delta E_g=0$, the calculated dependence of $\alpha(\omega)$ on doping concentration clearly disagrees with experiment in both n- and p-type GaAs. The positive Moss-Burstein shift is canceled by the negative band-gap shrinkage ΔE_g in real semiconductors.

In Fig. 8 we show the sensitivity of $\alpha(\omega)$ to $|M_{\text{env}}|^2$. The dashed line shows $\alpha(\omega)$ calculated using Eagles's constant ME given by (18). This ME describes electron excitation from a localized state right at the top of the valence band $E=E_v$ to a (delocalized state) right at the bottom of the conduction band. The (constant) $\alpha(\omega)$ in Fig. 8 is calculated using this fixed ME for all transitions, i.e., for all energies. The Eagles's ME describes $\alpha(\omega)$ quite well for $\hbar\omega<1.40$ eV, where transitions are indeed between the band edges, but overestimates $\alpha(\omega)$ at higher $\hbar\omega$. On the other hand, the parabolic ME, which is valid for completely delocalized states, describes $\alpha(\omega)$ well at high $\hbar\omega$ where transitions are indeed between delocalized states far from the band edges. The parabolic ME, given by (16), is used in $\alpha(\omega)$ together with parabolic bands having no band tails. The difference between the present full $\alpha(\omega)$ and the parabolic result shows the important contribution of band tailing to $\alpha(\omega)$ at low $\hbar\omega$.

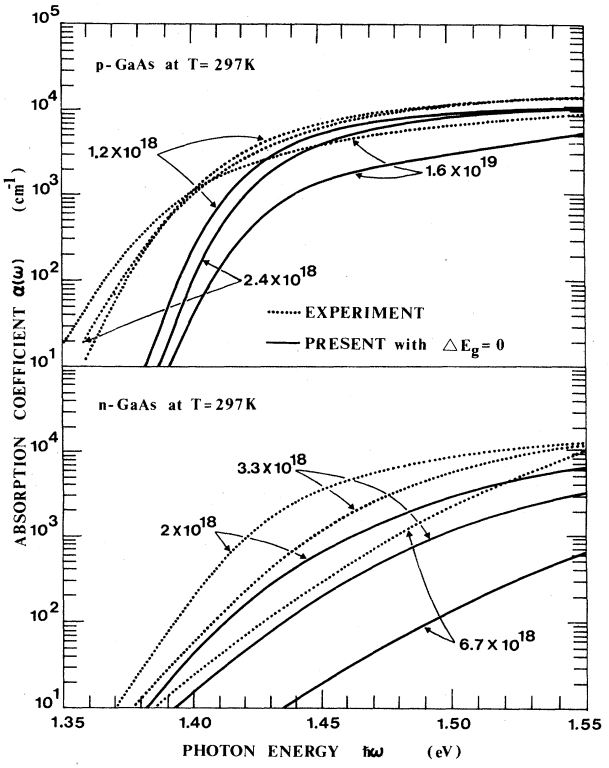

FIG. 7. Absorption coefficient in GaAs calculated (solid lines) using the present element, Eq. (15), and assuming a parabolic band above the mobility edge to determine k [Eq. (19)]. The band-gap shrinkage is set to zero ($\Delta E_g=0$). The dashed lines are the observed $\alpha(\omega)$ of Casey *et al.* (Ref. 8).

B. Optical absorption

In Fig. 9 we show the present $\alpha(\omega)$ calculated using the present matrix elements shown on Fig. 6 and Casey and Stern's[9] empirical expression for ΔE_g. The $\alpha(\omega)$ for three

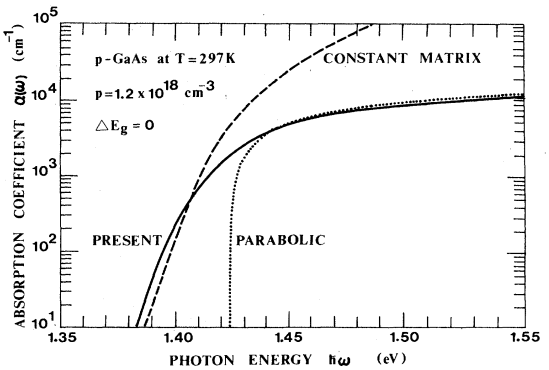

FIG. 8. Absorption coefficient calculated using (a) Eagle's constant matrix element (ME) (constant), (b) the ME in which all states are delocalized [Eq. (16)] (parabolic), and (c) the present ME [Eq. (15)] (present) all with $\Delta E_g=0$.

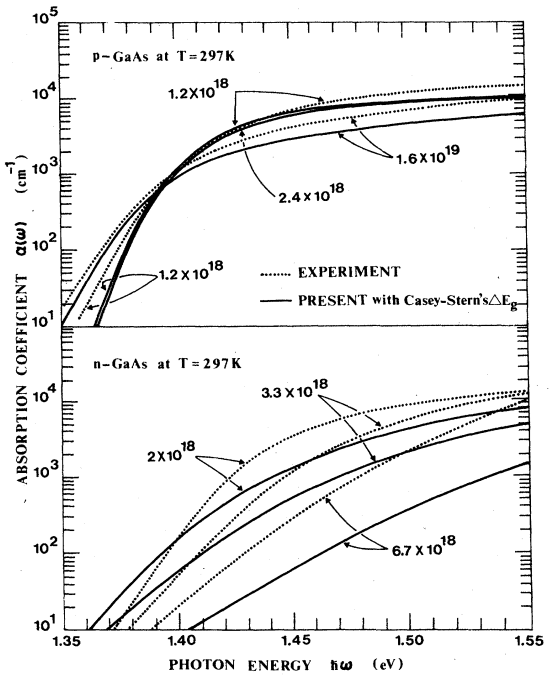

FIG. 9. Absorption coefficient calculated (solid lines) using the present theory with ΔE_g given by Casey and Stern's empirical expression (22) for both p- and n-type GaAs and with the mobility edge method for determining k. The dashed lines are the observed values of Casey *et al.* (Ref. 8).

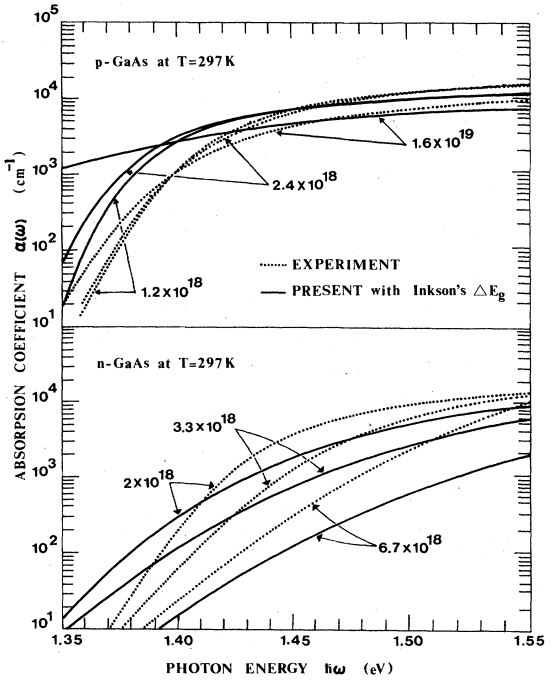

FIG. 10. As Fig. 9 with ΔE_g given by Inkson's Thomas-Fermi result.

doping concentrations of both n- and p-type GaAs is shown in Fig. 9. The values of ΔE_g used are listed in Table II. For n-type GaAs we have simply used Eq. (22) with p replaced by n. The mobility edge method is used to determine the values of k_v and k_c. The agreement with the observed $\alpha(\omega)$ is reasonably good at all energies $\hbar\omega$ in p-type GaAs. The agreement depends upon a complicated combination of the DOS, the screening, E_F, and E_g. The agreement is not as good for n-type GaAs. At low $\hbar\omega$, the calculated $\alpha(\omega)$ shows a much greater sensitivity to doping concentration than does the observed $\alpha(\omega)$, for example. At low $\hbar\omega$, $\alpha(\omega)$ is very sensitive to ΔE_g. This suggests that Casey and Stern's empirical rule for ΔE_g established for p-type GaAs cannot be simply translated to n-type GaAs with accuracy. In n-type GaAs, the calculated $\alpha(\omega)$ at high $\hbar\omega$ lies substantially below the observed values.

Figure 10 shows $\alpha(\omega)$ calculated as in Fig. 9 but using Inkson's[15] Thomas-Fermi expression (21) for ΔE_g. Comparing Figs. 9 and 10, $\alpha(\omega)$ is clearly very sensitive to ΔE_g at low $\hbar\omega$. Since Inkson's ΔE_g is a theoretical value, Fig. 10 is a more fundamental calculation of $\alpha(\omega)$. For p-type GaAs, the Inkson ΔE_g is clearly too large and gives an $\alpha(\omega)$ which lies to the left of the observed $\alpha(\omega)$ at low $\hbar\omega$. In this case, the Casey and Stern ΔE_g provides better agreement with experiment. However, for n-type the agreement with experiment is equally good (or poor) in Figs. 9 and 10. Comparing Figs. 9 and 10 we also see that $\alpha(\omega)$ is insensitive to ΔE_g at high $\hbar\omega$, as expected. Figures 9 and 10 represent the central results of the present paper.

IV. DISCUSSION

We review here the assumptions underpinning the present model of absorption and discuss their impact on $\alpha(\omega)$. The central assumption is the one-electron approximation; a photon is absorbed by exciting a single electron from a one-electron state in the valence band to a similar state in the conduction band. The $\alpha(\omega)$ in Eq. (1) contains an internally consistent treatment of the DOS [Eq. (3)], the envelope matrix element [Eq. (15)], the screening [Eq. (8)], and the Fermi energy [Eq. (7)]. The DOS is ob-

TABLE II. Values of band-gap shrinkage used in present calculations obtained using Inkson's formula (21) and Casey and Stern's empirical formula (22) for both p- and n-type GaAs.

p-type GaAs			n-type GaAs		
p (cm^{-3})	Inkson (meV)	Casey and Stern (meV)	n (cm^{-3})	Inkson (meV)	Casey and Stern (meV)
1.2×10^{18}	−34.9	−17.8	2×10^{18}	−33.7	−17.8
2.4×10^{18}	−45.8	−22.1	3.3×10^{18}	−40.0	−22.1
1.6×10^{19}	−93.8	−41.1	6.7×10^{18}	−50.8	−41.1

tained by evaluating the energy states available to a single electron interacting with randomly located, ionized impurities. Explicit electron-electron interactions are ignored. The impurity potentials seen by the electron are, however, screened by the other identical electrons. The screening is treated in a one-electron, Thomas-Fermi approximation. The screening length Q^{-1}, depends upon the DOS. The Fermi energy E_F depends upon both Q^{-1} and the DOS so that all three of E_F, Q^{-1}, and DOS are evaluated here iteratively until consistent.

The interaction between a single carrier and the impurities is represented by a screened Coulomb potential. The total potential seen by a carrier fluctuates as the concentration of impurities fluctuates throughout the sample. The fluctuating total potential is modeled by a nonlocal, harmonic well $[\frac{1}{2}m^*\omega^2 r^2(t)]$ which has a variable curvature $\omega^2(E)$. The $\omega(E)$ is treated as a variational parameter. The model ground-state wave function of the electrons (and holes) is therefore a Gaussian (see the Appendix). Thus we use Gaussian wave functions in the envelope matrix element [Eq. (15)], and once $\omega^2(E)$ is determined the parameters in the Gaussian electron (and hole) wave functions are fully established.

In Fig. 11 we show $\alpha(\omega)$ calculated using the present SG DOS given by (3) and using the Kane DOS. In both cases Eagles's constant matrix element is employed. The purpose of Fig. 11 is to display the sensitivity of $\alpha(\omega)$ to $\rho(E)$. We use Eagles's ME because the parameters γ_v and γ_c needed in the present ME [Eq. (15)] cannot be determined for Kane's DOS. As noted in Fig. 8 the $\alpha(\omega)$ at high photon energies $\hbar\omega$ in the "plateau region" is overestimated using Eagles's ME. However, Eagles's ME is quite accurate at low $\hbar\omega$ involving states near the band edges.

From Fig. 11 we see $\alpha(\omega)$ is very sensitive to $\rho(E)$. Kane's $\rho(E)$, which is too large in the band-tail region, clearly predicts an $\alpha(\omega)$ which is too large at low $\hbar\omega$. Also, Fig. 8 shows $\alpha(\omega)$ calculated using a parabolic DOS. In this case $\alpha(\omega)$ is too small at low $\hbar\omega$. Thus $\alpha(\omega)$ can clearly distinguish the SG from the Kane DOS and suggests the SG is, at least, approximately correct.

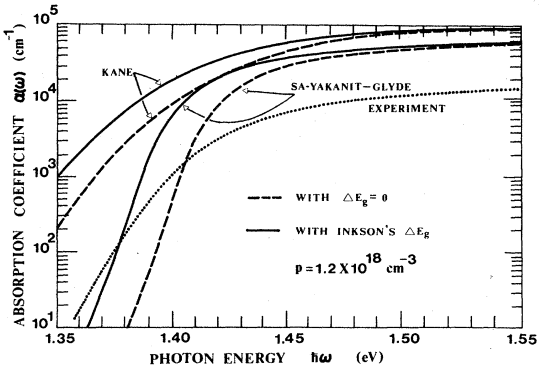

FIG. 11. Absorption coefficient calculated using the Kane and the Sa-yakanit and Glyde (SG) density of states in p-type GaAs. The dashed lines are for $\Delta E_g = 0$ and the solid lines for Inkson's ΔE_g. In all cases, Eagle's matrix element [Eq. (13)] is used.

However, at this stage, $\alpha(\omega)$ cannot be evaluated with enough confidence to distinguish between the SG and Halperin and Lax DOS, for example. The good agreement with experiment obtained for p-type GaAs shown in Fig. 9 therefore depends on an accurate band-tail DOS such as the SG or Halperin and Lax values.

As a further test of the DOS we compare the SG DOS calculated for p-type GaAs at 4.2 K with the observed values of Mahan and Conley in Fig. 12. In this case the screening length is $Q^{-1} = 1.99 \times 10^6$ cm^{-1}. Clearly, on the scale shown in Fig. 12 the agreement of the calculated and observed DOS's is good. The calculated and observed scales are set so that the parabolic DOS lies on the observed DOS at low energy. However, since the observed results are presented on a linear scale, they are not discriminating in the region $E - E_v \sim 100$ meV where important differences between models of band tailing occur. Any reasonable DOS such as Kane's DOS would agree with the observed value in Fig. 12.

From Fig. 8, $\alpha(\omega)$ is also clearly very sensitive to the envelope ME. The present ME [Eq. (15)] is a new ME which uses Gaussian envelope functions. It is algebraically much simpler and very different numerically from that developed by Casey and Stern who used hydrogenic envelope wave functions. The present ME, shown in Figs. 5 and 6, is relatively small in magnitude (the peak value is about one-tenth that of the Casey and Stern ME) but is a broad function spread over a wide energy interval. The Casey and Stern ME, in contrast, is a sharply peaked function of E. It is interesting that these two widely different ME's lead, when integrated over E in $\alpha(\omega)$, to very similar $\alpha(\omega)$ values as shown in Fig. 13. At high energy ($\hbar\omega \gtrsim 1.45$ eV) in the "plateau region" the two calculated $\alpha(\omega)$ agree closely, with the present value lying ~ 15–20% above Casey and Stern's value. At low $\hbar\omega$, the difference between the present and Casey and Stern values of $\alpha(\omega)$ shown in Fig. 11 is due almost entirely to the different values of ΔE_g used. The present $\alpha(\omega)$ used ΔE_g from (21) while Casey and Stern used (22). If we had used (22), the two $\alpha(\omega)$ would lie nearly on top of one another at low $\hbar\omega$ (see Fig. 9). In the present case, once the DOS is established, the envelope ME is completely determined and there is no further adjustment possible. Clearly the combined SG DOS and the present ME lead

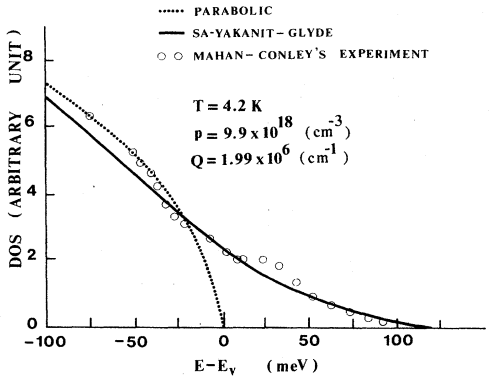

FIG. 12. SG and parabolic density of states compared with the observed values of Mahan and Conley (Ref. 26).

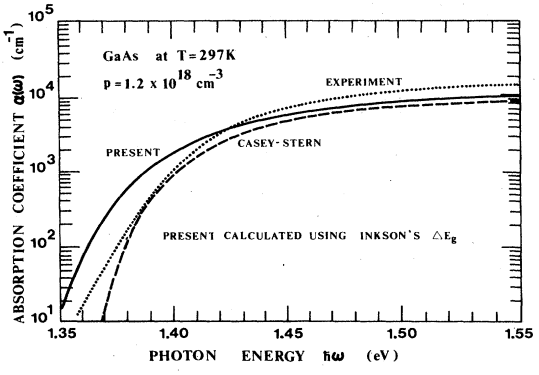

FIG. 13. Comparison of (a) present $\alpha(\omega)$ (solid line) calculated using Inkson's ΔE_g and the mobility edge method of determining k with (b) Casey and Stern's (Ref. 9) calculated $\alpha(\omega)$ (dashed line) and (c) experiment (dotted line) (Ref. 8).

to a very reasonable value of $\alpha(\omega)$.

The $\alpha(\omega)$ is also sensitive to the value of E_F. This sensitivity appears at low $\hbar\omega$; as E_F increases, $\alpha(\omega)$ is shifted to the right (the Moss-Burstein shift). E_F is proportional to the doping concentration as shown in Fig. 7. As noted above the increase in E_F with doping competes with the shrinkage of the band gap ΔE_g, which is opposite in sign and larger in magnitude than E_F. Thus it is difficult to isolate the precise impact of E_F in comparing the calculated $\alpha(\omega)$ with experiment.

To test the sensitivity of $\alpha(\omega)$ to the band-gap shrinkage ΔE_g we evaluated $\alpha(\omega)$ using ΔE_g given by Casey and Stern's empirical expression and as calculated by Inkson. The two $\alpha(\omega)$ are shown in Figs. 9 and 10, respectively. The $\alpha(\omega)$ is clearly very sensitive to ΔE_g. As discussed by Mahan,[34] by Berggren and Sernelius,[35] and by Sterne and Inkson,[36] ΔE_g is difficult to evaluate with accuracy and improved values will certainly appear in the future. Inkson's ΔE_g appears to be too large and this displaces the calculated $\alpha(\omega)$ well to the left of the observed $\alpha(\omega)$ at low $\hbar\omega$. Inkson's ΔE_g is probably too large because the Thomas-Fermi approximation overestimates the screening. A better treatment of screening will bring ΔE_g back closer to the unscreened values (see Fig. 4). Thus the present values of $\alpha(\omega)$ shown in Fig. 10 are uncertain and subject to change with ΔE_g.

Also, we have ignored the electron-hole interaction throughout the present calculation. This interaction should be small since it is strongly screened by the added electrons in the conduction band when GaAs is heavily doped. However, there may be a remnant of it (particularly at large compensation ratios). Since it is attractive, it would lead to an apparent reduction of E_g.

As noted in Figs. 5 and 6, the ME is not very sensitive to the way in which k_v and k_c are determined. The simpler mobility edge method may therefore be preferable. However, the actual values assigned for the mobility edges E_{mc}, E_{mv} in this method is somewhat arbitrary ($E_{mv}=0, E_{mc}=E_g$). If E_{mc} is increased, for example, the magnitude of $\alpha(\omega)$ increases at high $\hbar\omega$ in the plateau region but $\alpha(\omega)$ changes little at low $\hbar\omega$. For a 15% increase in E_{mc}, the plateau of $\alpha(\omega)$ in Fig. 9 increases by $\sim 50\%$ to lie just above the observed $\alpha(\omega)$. For $E_{mc} > 1.15E_g$, all the conduction-band states become localized within the energy range covered in Fig. 9 and $\alpha(\omega)$ cannot increase further.

We have chosen the heavy-hole valence-band mass as $m_{hh}=0.55m_0$ to conform with the value used by Casey and Stern.[9] We could equally well have used the value $m_{hh}=0.68m_0$ proposed by Ehrenreich.[41] We found changing m_{hh} from 0.55 to 0.68 changed $\alpha(\omega)$ little (10—20 % in the plateau region) so that $\alpha(\omega)$ is not greatly sensitive to m_{hh}. We regard the $\alpha(\omega)$ shown in Fig. 9 as our best and final result for $\alpha(\omega)$. Is the difference between the calculated $\alpha(\omega)$ and experiment shown in Fig. 9 significant? In the plateau region of $\alpha(\omega)$ lies ~ 40—50% below experiment. As noted above this difference could be removed by a slight adjustment of the mobility edge. Indeed, given the great sensitivity of $\alpha(\omega)$ to the ME and the DOS, both of which are unadjusted, the agreement with experiment is very good. At low ω, the energy ($\hbar\omega$) at which $\alpha(\omega)$ becomes significant depends critically on ΔE_g, on E_F, and on the density of states. Given that ΔE_g is not well determined, we cannot attribute much significance to the difference between the calculated and observed $\alpha(\omega)$ at low photon energy. Particularly, the apparent band gap depends on a sensitive cancellation between E_F and ΔE_g.

Note added in proof: Recent measurements [L. G. Shantharama *et al.*, J. Phys. C **17**, 4429 (1984)] suggest m_b^2 in (12) should be close to its original value without the factor of 1.25.

ACKNOWLEDGMENTS

We are grateful to Dr. Frank Stern for many helpful discussions and incisive comments on this work. We wish to acknowledge the Canadian International Development Agency and the Unit Cell Project of Chulalongkorn University for financial support.

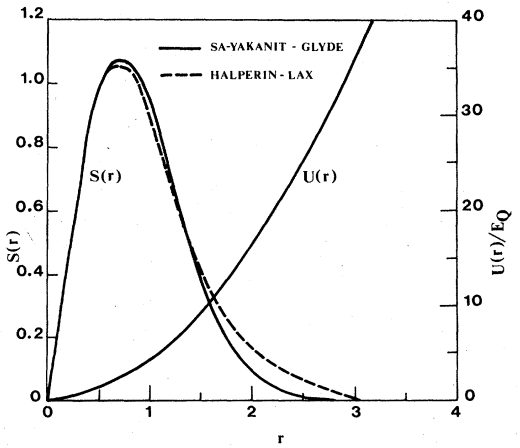

FIG. 14. Parabolic impurity potential $U(r)$ and wave function $S(r)$ of an electron in the potential $U(r)$.

APPENDIX

In this appendix we illustrate how the Gaussian envelope functions, Eq. (14), which describe particles in the band tail, follow naturally as the appropriate localized functions to accompany the SG theory of the DOS. Firstly, the SG theory employs the Feynman path-integral method. It is well known that the propagator G in this method is related to the wave function $\Phi_n(x)$ by

$$G(xt,x't')=\sum_n \Phi_n(x)\Phi_n(x')e^{-(1/\hbar)E_n(t-t')} . \quad \text{(A1)}$$

Secondly, to evaluate the first-order energies, such as the ME in (1), it is sufficient to use only a zero-order wave function. Thus we need only a zero-order propagator in (A1).

In the SG theory the potential seen by a carrier electron due to impurities is modeled by a harmonic well having variable curvature ($m\omega$). The zero-order propagator needed is therefore that for a free particle in a harmonic well.[5,6] This is obtained from (A1) if the $\Phi_n(x)$ are harmonic oscillator (HO) wave functions and the E_n are HO energies. This G_0 can be evaluated readily in closed form.[4–6,42] For localized electrons deep in the band tail, only the ground states[20,5] of the HO's are retained. Thus

$$G_0(xt,x't')=\Phi_0(x)\Phi_0^*(x')e^{-i\omega(t-t')} , \quad \text{(A2)}$$

where

$$\Phi_0(x)=\left[\frac{m\omega}{\pi\hbar}\right]^{3/4}\exp\left[-\frac{1}{2}\left[\frac{m\omega}{\hbar^2}\right]x^2\right] . \quad \text{(A3)}$$

These are the Gaussian envelope functions used in (14) with variational parameter $\gamma=m\omega/2\hbar=Q^2/2z^2$. The value of ω was determined as a function of electron energy using the Lloyd and Best[21] variational principle.

This Gaussian function may be compared with the wave function $S(r)$ determined by Halperin and Lax, which is related to Φ_0 by

$$S(r)=\sqrt{4\pi}r\Phi_0(r) . \quad \text{(A4)}$$

In Fig. 14 we compare our Gaussian $S(r)$ obtained[7] from (A4) for $z=0.7059$, $\nu=10$, and $Q=1$ with that of Halperin and Lax. Also plotted in Fig. 14 is the model harmonic well $U(r)/E_Q=\frac{1}{2}m^*\omega^2r^2/E_Q$ in units of $E_Q=H^2Q^2/2m^*$. Figure 14 shows that the general numerical $S(r)$ obtained by Halperin and Lax is nearly Gaussian.

*Permanent address: Physics Department, Chulalongkorn University, Bangkok 10500, Thailand.

[1]R. A. Abram, G. J. Rees, and B. H. L. Wilson, Adv. Phys. **27** 799 (1978).
[2]D. Redfield, Adv. Phys. **24**, 463 (1975).
[3]A. L. Efros, Usp. Fiz. Nuak. **111**, 451 (1973) [Sov. Phys.—Usp. **16**, 789 (1974)].
[4]V. Sa-yakanit (or Samathiyakanit), J. Phys. C **7**, 2849 (1974).
[5]V. Sa-yakanit, Phys. Rev. B **19**, 2266 (1979).
[6]V. Sa-yakanit, and H. R. Glyde, Phys. Rev. B **22**, 6222 (1980).
[7]V. Sa-yakanit, W. Sritrakool, and H. R. Glyde, Phys. Rev. B **25**, 2776 (1982).
[8]H. C. Casey, Jr., D. D. Sell, and K. W. Wecht, J. Appl. Phys. **46**, 250 (1975).
[9]H. C. Casey, Jr. and F. Stern, J. Appl. Phys. **47**, 631 (1976).
[10]R. J. Archer, R. C. C. Leife, A. Yariv, S. P. S. Porto, and J. M. Wehlan, Phys. Rev. Lett., **10**, 453 (1963).
[11]J. I. Pankove, Phys. Rev. **140**, 2059 (1965).
[12]P. A. Wolff, Phys. Rev. **126**, 405 (1962); Proceedings of the International Conference on the Physics of Semiconductors, Exeter, 1962 (unpublished), p. 220.
[13]W. F. Brinkman and P. A. Lee, Phys. Rev. Lett. **31**, 237 (1973).
[14]D. C. Herbert, D. T. J. Hurle, and R. M. Logan, J. Phys. C **8**, 3571 (1975).
[15]J. C. Inkson, J. Phys. C **6**, 1350 (1973); **9**, 1177 (1976).
[16]T. S. Moss, Proc. Phys. Soc. B **67**, 775 (1967).
[17]E. Burstein, Phys. Rev. **93**, 632 (1957).
[18]E. O. Kane, Phys. Rev. **131**, 79 (1963).
[19]V. L. Bonch-Bruevich, Fiz. Tverd. Tela (Leningrad) **4**, 2660 (1962) [Sov. Phys.—Solid State **4**, 1953 (1963)].
[20]B. I. Halperin and M. Lax, Phys. Rev. **148**, 722 (1966); **153**, 802 (1967).
[21]P. Lloyd and R. P. Best, J. Phys. C **8**, 3752 (1975).
[22]W. Sritrakool, H. R. Glyde, and V. Sa-yakanit, Can. J. Phys. **60**, 373 (1982).
[23]G. D. Mahan and J. W. Conley, Appl. Phys. Lett. **11**, 29 (1967).
[24]M. Takeshima, Phys. Rev. B **27**, 2387 (1983).
[25]F. Stern, in *Solid State Physics,* edited by H. Ehrenreich, F. Seitz, and D. Turnbull (Academic, New York, 1963), Vol. 15, p. 299.
[26]G. Lasher and F. Stern, Phys. Rev. **133**, 553 (1964).
[27]W. Kohn, in *Solid State Physics,* edited by H. Ehrenrich, F. Seitz, and D. Turnbull (Academic, New York, 1957), Vol. 5, p. 257.
[28]E. O. Kane, J. Phys. Chem. Solids **1**, 249 (1957).
[29]D. J. Chadi, A. H. Clark, and R. D. Burnham, Phys. Rev. B **13**, 4466 (1976); C. Hermann and C. Weisbuch, *ibid.* **15**, 823 (1977).
[30]D. W. Eagles, J. Phys. Chem. Solids **16**, 76 (1960).
[31]W. Sritrakool, Ph.D. thesis, University of Ottawa, 1984.
[32]P. W. Anderson, Phys. Rev. **109**, 1492 (1958).
[33]J. C. Phillips, Philos. Mag. B **47**, 407 (1983).
[34]G. D. Mahan, J. Appl. Phys. **51**, 2634 (1980).
[35]K. F. Berggren and B. E. Sernelius, Phys. Rev. B **24**, 1971 (1981).
[36]P. A. Sterne and J. C. Inkson, J. Appl. Phys. **52**, 6432 (1981).
[37]C. J. Hwang, Phys. Rev. B **2**, 4117 (1970); **2**, 4126 (1970); J. Appl. Phys. **41**, 2668 (1970).
[38]C. J. Hwang and J. R. Brews, J. Phys. Chem. Solids **32**, 837 (1970).
[39]D. Auverge, J. Camassel, and H. Mathieu, Phys. Rev. B **11**, 2251 (1975).
[40]J. Serre, A. Ghazali, and P. Leroux Hugon, Phys. Rev. B **23**, 1971 (1981).
[41]H. Ehrenreich, Phys. Rev. **120**, 1951 (1963).
[42]R. P. Feynman and A. R. Hibbs, *Quantum Mechanics and Path Integrals* (McGraw-Hill, New York, 1965).